Assessment of the Shear Capacity of Existing Reinforced Concrete Solid Slab Bridges

By

Eva O.L. Lantsoght, PhD Candidate, Delft University of Technology, Department of Design & Construction – Concrete Structures, St II 2.06, Stevinweg 1, 2628 CN Delft, The Netherlands, 0031 15 2787449, E.O.L.Lantsoght@tudelft.nl (corresponding author),

Cor van der Veen, Associate Professor, Delft University of Technology, Department of Design & Construction – Concrete Structures, St II 2.05, Stevinweg 1, 2628 CN Delft, The Netherlands, 0031 15 2784577, C.vanderveen@tudelft.nl,

Joost C. Walraven, Full Professor, Delft University of Technology, Department of Design & Construction – Concrete Structures, St II 2.02, Stevinweg 1, 2628 CN Delft, The Netherlands, 0031 15 2785452, J.C.Walraven@tudelft.nl, and

Ane de Boer, Senior Adviser, Ministry of Infrastructure and the Environment, Department of Infrastructure, Section of Civil Engineering H13, P.O. Box 20.000, 2502LA Utrecht, The Netherlands, ane.de.boer@rws.nl

Submission Date: 23/10/2012

Word Count: 5076 words (text) + 2000 word equivalents (3 tables and 5 figures) = 7076 words

Assessment of the Shear Capacity of Existing Reinforced Concrete Solid Slab Bridges

ABSTRACT

Several existing reinforced concrete solid slab bridges in the Netherlands do not meet the criteria for shear when calculated according to the recently implemented Eurocodes. The shear capacity is assessed by comparing the design beam shear resistance to the design value of the applied shear force due to the dead load, permanent load and live load. Transverse load redistribution which occurs in slabs is not taken into account. To evaluate a large number of slab bridges, a first round of assessments is necessary to determine which bridges need a more detailed shear analysis.

A series of 26 slabs and 12 slab strips are tested until shear failure. The results of these experiments are compared to the state-of-the-art in beam shear research to compare the shear behavior of beams and slabs. Recommendations for the shear assessment of slabs are formulated, and used to verify the shear capacity of 10 cases of slab bridges. This “Quick Scan” approach is compared to the AASHTO provisions, which are found to be less conservative. However, the underlying target reliability index is significantly smaller for the AASHTO provisions.

For the existing bridges in the Netherlands, the proposed method can analyze a large number of cross-sections and thus help prioritize the efforts of the owners such that cases which need a more detailed shear analysis are identified.

INTRODUCTION

In the Netherlands, a large number of the existing reinforced concrete bridges in the road network are short span solid slab bridges, 60% of which are built before 1975. When these bridges are assessed for shear according to the current codes, they are often found not to satisfy the criteria for two reasons. First, the traffic loads and volumes have increased over the past decades, resulting in heavier load models prescribed by the recently implemented Eurocodes. Second, the shear provisions have become more conservative. However, no signs of distress can be observed on these structures (*1*).

The Dutch Ministry of Infrastructure and the Environment initiated a project to assess the capacity of existing bridges under the increased live loads. Amongst others, the shear capacity of 600 slab bridges should be studied (*2*). A first round of assessments aims at determining which bridges require a more detailed shear analysis. For this purpose, a fast, simple and conservative tool is required. The "Quick Scan" method is developed, which results in a "unity check" value. The unity check gives the ratio between the design value of the applied shear force resulting from the composite dead load and live loads on the bridge according to current codes and the shear resistance. The Quick Scan aims at determining the unity check near the edge, as a design truck near the edge is identified as the critical loading case (*3*).

Typically, the shear capacity of one-way slabs and slab bridges is determined by considering a slab as a beam with a large width. The beam shear capacity is derived from experiments on small, heavily reinforced beams. Extrapolating these results to the shear capacity of slabs might be overly conservative as transverse redistribution of stresses can occur in slabs. Experimental results on decommissioned slab bridges indicated that these bridges possess a much higher residual shear capacity (*4, 5, 6*).

LITERATURE REVIEW

Shear Capacity of Reinforced Concrete Slabs

Shear Provisions in Codes and Effective Width

This study is based on the beam shear provisions of EN 1992-1-1:2005 (*7)* and AASHTO LRFD (*8)*. EN 1992-1-1:2005 (*7)* uses an empirical formulation based on a statistical analysis (*9)*. The shear provisions in AASHTO LRFD are based on the modified compression field theory (*10*). For slabs and wide beams under concentrated loads, the effective width is used in the expressions for the shear capacity. This width can be determined from a horizontal load spreading method. Theoretically, the effective width b_{eff} is determined in such a way that the total shear stress over the support equals the maximum shear stress over the effective width. In practice, a method of horizontal load spreading is chosen, Fig. 1, depending on local practice. In Dutch practice, horizontal load spreading is assumed under a 45° angle from the center of the load towards the support (Fig. 1a). In French practice (*11*), load spreading is assumed under a 45° angle from the far corners of the loading plate towards the support (Fig. 1b).

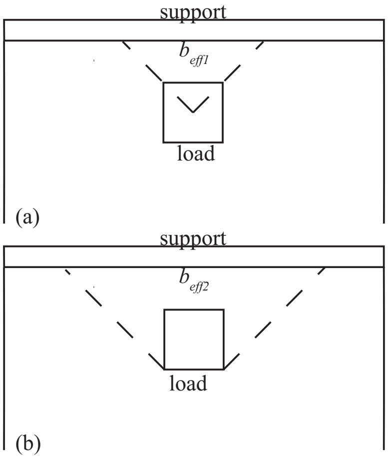

FIGURE 1 Top view of slab showing determination of effective width (a) assuming 45º horizontal load spreading from the center of the load: b_{eff1}; (b) assuming 45º horizontal load spreading from the far corners of the load: b_{eff2}.

Available Experimental Data

Recent experimental research (*12*) concerning shear in slabs has mainly focused on one-way slabs under line loads. These experiments proved that one-way slabs under line loads behave like beams, with beam shear provisions leading to good estimates of their capacity. A database of 215 experiments on wide beams and slabs (*13*) shows that data of shear tests on one-way slabs under a concentrated load are scarce. Experiments with a concentrated load close to the support are of interest to study the case in which the design truck is near to the support, resulting in high shear forces at the face of the support. Only 22 experiments with a (the center-to-center distance between the load and the support) of less than $2.5d_l$ (the effective depth) are available (*14-17)*, the majority of which are carried out on small specimens (d_l < 15cm = 5.9in).

Live Load Models

In EN 1991-2:2003 (*18)* load model 1, a design truck is combined with a design lane load. The design truck has a tire contact area of 400mm × 400mm (15.7in × 15.7in) and an axle load of α_{Q1} × 300kN (67kip) in the first lane, α_{Q2} × 200kN (45kip) in the second lane and α_{Q3} × 100kN (23kip) in the third lane. All α_{Qi} equal 1. The lane load is applied over the full width of the lane and equals α_{q1} × 9kN/m^2 (1.31psi) for the first lane and α_{qi} × 2.5kN/m^2 (0.36psi) for all other lanes. The values of α_{qi} are given in the National Annex. In the Netherlands, for bridges with 3 or more notional lanes, the value of α_{q1} equals α_{q1} = 1.15 and for i > 1 α_{qi} = 1.4.

In AASHTO LRFD (*8)* a combination of a design truck or tandem with a design lane load is considered. The tire contact area is 510mm × 250mm (20in × 10in) for design truck and tandem. The design truck has 3 axle loads: 35kN (8kip) and two times 145kN (32kip). The design tandem consists of a pair of 110kN (25kip) axles. A dynamic load allowance has to be considered for both the wheel loads. For the limit state of strength for concrete slabs, the dynamic allowance *IM* equals 33% (Table 3.6.2.1-1 from AASHTO LRFD). The design lane load from AASHTO LRFD (*8*) consists of a load of 9.3N/mm (0.64klf) transversely distributed over a 3000mm (10ft) width, which is smaller than the full lane width (3.6m = 12ft).

Assessment Practice

Currently, the Eurocode suite only provides load factors for design. The Eurocodes for assessment are under preparation. For assessment according to the philosophy of the Eurocodes, in the Netherlands a set of national codes (NEN 8700 for the basic rules, NEN 8701 for actions, NEN 8702 for concrete structures etc.) is developed. Three safety levels are defined in NEN 8700:2011 (*19*): "new", "repair" and "unfit for use". The Ministry of Infrastructure and the Environment of the Netherlands has decided to rate the existing slab bridges for shear at the "repair" level. For "repair" level, consequences class 3 (high consequence for the loss of human life or very great economic, social or environmental consequences, EN 1990:2002 (22) Table B1), a reliability index β_{rel} = 3.6 is required (*20, 21*). The load factors are given in NEN 8700:2011 Table A1.2(B) and (C): γ_{DL} = 1.15 is used for dead loads and γ_{LL} = 1.3 for live loads.

For load and resistance factor rating (LRFR) according to the AASHTO Manual of Bridge Evaluation (MBE) (*23*), the factors for design load at the operating level are used, describing the maximum permissible live load to which the structure may be subjected. The definition of the operating level is thus similar to the "repair" level from NEN 8700:2011. In Table 6.A.4.2.2.-1 the load factors are given as γ_{DL} = 1.25 for the dead load, γ_{DC} = 1.50 for the superimposed loads and γ_{LL} = 1.35 for the live loads. The target reliability index of these factors is β_{rel} = 2.5 and is thus considerably lower than the reliability index related to the Dutch "repair" level (*24*). Moreover, for concrete slabs and slab bridges designed in conformance with AASHTO specifications, the shear capacity can be considered as satisfactory (*23*). Also, shear need not be checked for design load and legal load rating of concrete members (*23*).

EXPERIMENTS

Experimental Setup

To improve the assessment of slab bridges under live loads, the transverse load distribution and effective width need to be determined. For this purpose, a series of experiments on the shear capacity of slabs under concentrated loads is executed on a half-scale model of a continuous reinforced concrete slab bridge. The test program consists of 26 slabs (S-series) of 5m × 0.3m × 2.5m (16ft × 1ft × 8ft) and 12 slab strips (B-series) of 5m × 0.3m (16ft × 1ft) on which a total of 156 experiments are carried out. A top view of the test setup is presented in Fig. 2. The support conditions are varied: slabs on line supports, 3 elastomeric bearings per support or 7 bearings per support (elastomeric or steel) are tested. S1 to S18 and all slab strips (BS1 to BX3) are tested with a concentrated load only; S19 to S26 are tested under a combination of a concentrated load and a line load of 240kN/m (16.5kip/ft) at 1.2m (4ft) from the support. Experiments are carried out close to the simple support (sup 1, SS in Fig. 2) and the continuous support (sup 2, CS in Fig. 2), where the rotation is partially restrained by vertical prestressing bars. The concentrated load is placed at different positions along the span of the slab: at a center-to-center distance between the load and the support *a* of 400mm (15.7in) and 600mm (23.6in); and at different positions along the width: in the middle ("M" in Fig. 2) and near the edge of the slab ("E" in Fig. 2). The size of the concentrated load is taken as 200mm × 200mm (7.9in × 7.9in) (half-scale of the tire contact area used in EN 1991-2:2003 (*18*) as the scale of the experiment is 1:2) or as 300mm × 300mm (11.8in × 11.8in).

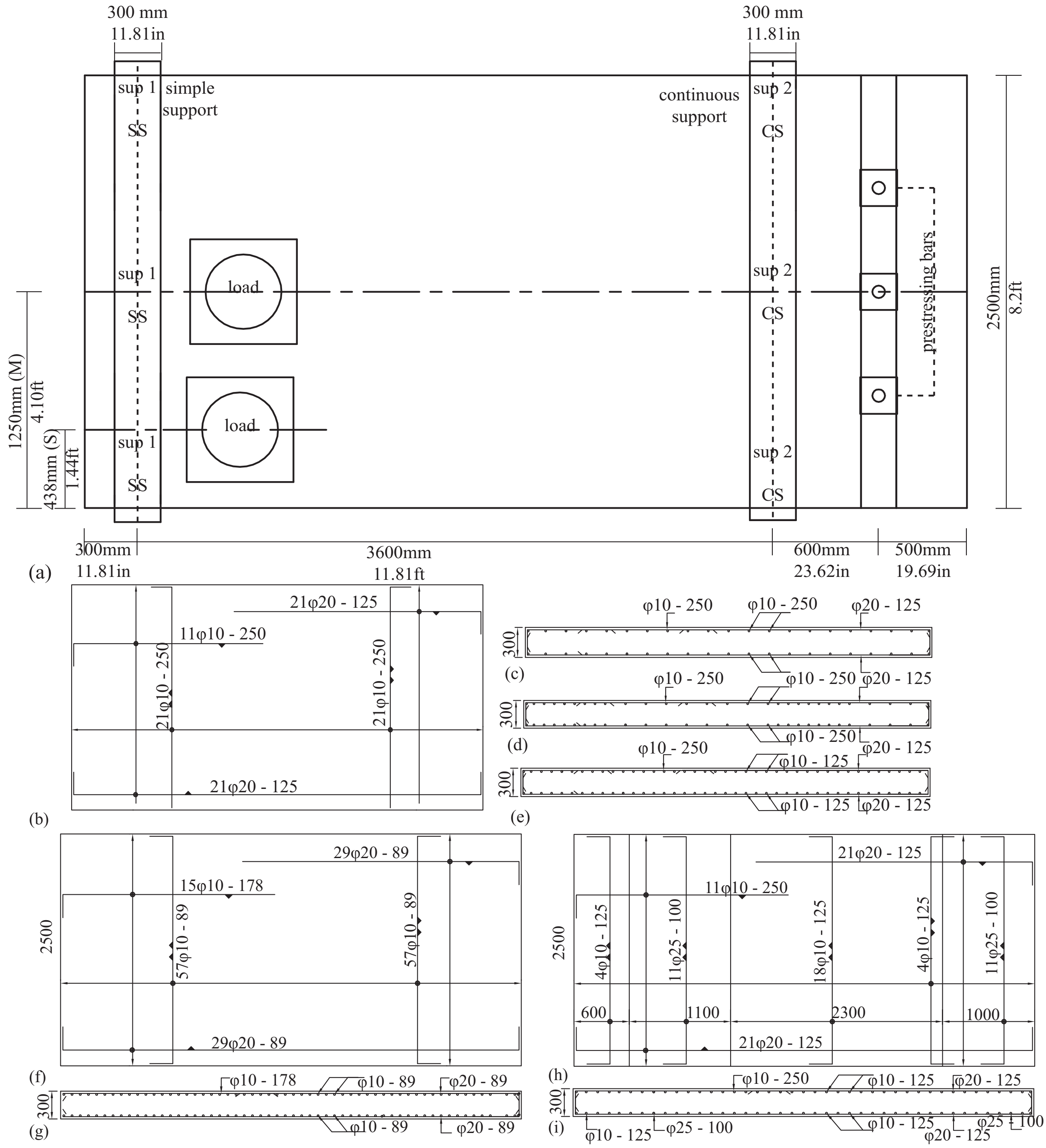

FIGURE 2 Experimental setup and specimens: (a) top view of setup, (b) top view and (c) cross-section of reinforcement layout for S1, S2; (d) cross-section of S4; (e) cross-section of S3, S5-S10, S19-S26; (f) top view and (g) cross-section of S11-S14; (h) top view and (i) cross-section of S15-s18.

Specimens and Results

All specimens are cast at Delft University of Technology. During each cast, two specimens with identical properties are made. The following parameters are varied in the specimens: the amount of transverse flexural reinforcement (0.132% Fig. 2c, 0.182% Fig. 2d and 0.258%, Fig. 2e), the concrete compressive strength (normal strength and high strength concrete), plain bars as compared to deformed bars and, in the B-series, the overall specimen width (BS/0.5m = 1.6ft, BM/1m = 3.3ft, BL/1.5m = 4.9ft and BX/2m = 6.6ft). All specimens have a cross-sectional depth *h* of 300mm (11.8 in). Slabs S1 to S14 and S19 to S26 (Fig. 2b,f) and all slab strips BS1 to BX3 have an effective depth to the main flexural reinforcement d_l of 265mm (10.4in). Slabs S15 to S18 (Fig. 2h,i), on 3 elastomeric bearings per support, have an effective depth d_l of 255 mm (10in), as increased cover was required for the virtual beam in the transverse direction above the support. The properties of the studied specimens are given in Table 1, with:

b the width of the specimen;
f_c' the cube compressive strength at the age of testing;
f_{ct} the splitting tensile strength at the age of testing;
ρ_l the amount of longitudinal reinforcement;
ρ_t the amount of transverse flexural reinforcement;
a/d the shear span to depth ratio;
M/E location of the concentrated load along the width (Fig. 2a);
z_{load} the size of the loading plate;
age the age of the specimen at testing.

Further discussion of the individual tests of S1 to S10 and the slab strips (*25*), S11 to S14 (*26*) and S15 to S26 (*27*) are reported elsewhere.

COMPARISON BETWEEN SLABS AND BEAMS

The results of the experiments on slabs are compared to the state-of-the-art with regard to beam shear (*25*). To understand the differences between slabs and beams in shear, and the benefit of transverse load redistribution in slabs, the main findings of the parameter analysis are given in this section.

Reinforced concrete slabs loaded with a concentrated load close to the support show a three-dimensional behavior which is distinctly different from the two-dimensional shear carrying behavior in beams, as represented by the cracking pattern at the bottom of a tested specimen, Fig. 3. Three-dimensional load bearing behavior is experimentally observed for the following parameters: size of the loading plate, moment distribution in the shear span, distance between load and support, concrete compressive strength and the results of the specimen width.

The influence of the shear span to depth ratio is experimentally observed to decrease for an increase in specimen width, which can be explained by compressions struts. While for beams, a clearly defined strut develops over the distance *a*, in slabs, a fan of struts can develop, Fig. 3c. In beams, only the straight strut (a/d_l = 1 in Fig. 3c) can develop. In slabs, the a/d_l will be influenced by the fan of struts and their resulting load path. A larger average a/d_l results, leading to a smaller influence of a/d_l on the shear resistance of slabs. Again, the behavior of beams and slab strips with two-dimensional load-carrying behavior differs from slabs with three-dimensional load-carrying behavior.

The experimental results indicate that for slabs, the influence of the moment distribution over the support is smaller than for beams. Also, the effective width calculated from the measured reaction forces by load cells at the support is smaller at the continuous than at the simple support. The results of linear finite element calculations yield similar conclusions with regard to the moment distribution, indicating no influence of cracking or force redistribution but solely the action of forces and moments. These observations indicate that for slabs failing in shear the transverse moment should be taken into account.

TABLE 1 Properties of tested specimens. Note: 1m = 3.28ft, 1mm = 0.04in., 1MPa = 0.145ksi

Slab nr.	***b*** **(m)**	**f_c' (MPa)**	**f_{ct} (MPa)**	**ρ_l (%)**	**ρ_t (%)**	***a/d***	**M/E**	**z_{load} (mm)**	**age (days)**
S1	2.5	35.8	3.1	0.996	0.132	2.26	M	200	28
S2	2.5	34.5	2.9	0.996	0.132	2.26	M	300	56
S3	2.5	51.6	4.1	0.996	0.258	2.26	M	300	63
S4	2.5	51.7	4.2	0.996	0.182	2.26	E	300	76
S5	2.5	48.2	3.8	0.996	0.258	1.51	M	300	31
S6	2.5	50.6	3.9	0.996	0.258	1.51	E	300	41
S7	2.5	82.1	6.2	0.996	0.258	2.26	E	300	83
S8	2.5	77.0	6.0	0.996	0.258	2.26	M	300	48
S9	2.5	81.7	5.8	0.996	0.258	1.51	M	200	77
S10	2.5	82.4	5.8	0.996	0.258	1.51	E	200	90
S11	2.5	54.9	4.2	1.375	0.358	2.26	M	200	90
S12	2.5	54.8	4.2	1.375	0.358	2.26	E	200	97
S13	2.5	51.9	4.2	1.375	0.358	1.51	M	200	91
S14	2.5	51.3	4.2	1.375	0.358	1.51	E	200	110
S15	2.5	52.2	4.2	1.035	1.078	2.35	M	200	71
S16	2.5	53.5	4.4	1.035	1.078	2.35	E	200	85
S17	2.5	52.5	3.7	1.035	1.078	1.57	M	200	69
S18	2.5	52.1	4.5	1.035	1.078	1.57	E	200	118
S19	2.5	56.9	4.7	0.996	0.258	2.26	M	300	89
S20	2.5	60.5	4.7	0.996	0.258	2.26	M	var	176
S21	2.5	56.8	4.5	0.996	0.258	2.26	M	300	187
S22	2.5	58.0	4.5	0.996	0.258	2.26	E	300	188
S23	2.5	58.9	4.7	0.996	0.258	2.26	M	300	197
S24	2.5	58.9	4.7	0.996	0.258	2.26	E	300	183
S25	2.5	58.6	4.5	0.996	0.258	var	M	300	170
S26	2.5	58.6	4.5	0.996	0.258	1.51	M&E	300	174
BS1	0.5	81.5	6.1	0.996	0.258	2.26	M	300	55
BM1	1	81.5	6.1	0.996	0.258	2.26	M	300	62
BL1	1.5	81.5	6.1	0.996	0.258	2.26	M	300	189
BS2	0.5	88.6	5.9	0.996	0.258	1.51	M	200	188
BM2	1	88.6	5.9	0.996	0.258	1.51	M	200	188
BL2	1.5	94.8	5.9	0.996	0.258	1.51	M	200	180
BS3	0.5	91.0	6.2	0.996	0.258	2.26	M	300	182
BM3	1	91.0	6.2	0.996	0.258	2.26	M	300	182
BL3	1.5	81.4	6.2	0.996	0.258	2.26	M	300	171
BX1	2	81.4	6.0	0.996	0.258	2.26	M	300	47
BX2	2	70.4	5.8	0.996	0.258	1.51	M	200	39
BX3	2	78.8	6.0	0.996	0.258	2.26	M	200	40

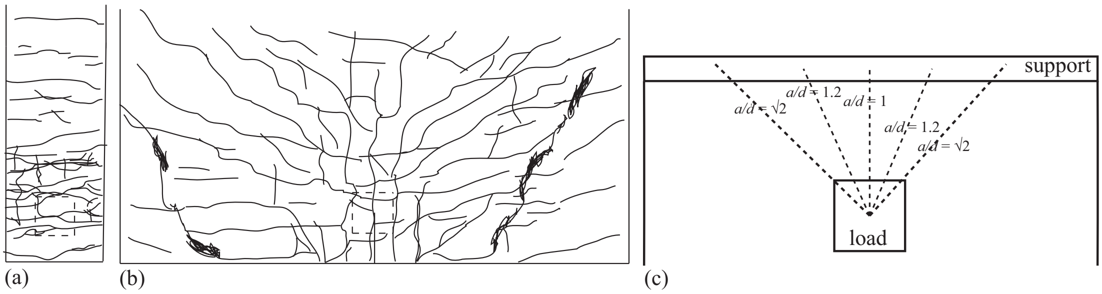

FIGURE 3 Aspects of horizontal load redistribution: (a) cracking pattern at bottom face after BS2T1; (b) cracking pattern at bottom face after S9T1, showing three-dimensional load bearing behavior. The dashed lines denote the location of the loading plate. Thicker lines in (b) denote areas of punching damage; (c) fanning of compression struts leading to larger average a/d_l ratio for slabs as compared to beams.

It is experimentally observed that the increase in shear capacity for an increase in the size of the loading plate increases for increasing specimen widths. This observation can be explained based on transverse load redistribution. Considering the load distribution from the concentrated load towards the support in a slab as a three-dimensional problem in which compression struts occur over the depth and the width of the slab, a larger loading plate provides a larger base for fanning out compressive struts. As these compressive struts develop over a larger area, more material is activated to carry the load, thus increasing the shear capacity. For members with a smaller width, transverse load redistribution cannot develop. In this case, the size of the loading plate should not influence the capacity of the member.

QUICK SCAN APPROACH

Recommendations

The experimental results led to recommendations for the effective width of the wheel loads, transverse stress redistribution and superposition of loads.

Choice of Effective Width

The results of the series of slab strips are used to evaluate the horizontal load spreading methods. Applying the concept of an effective width, increasing the width should show equally increasing ultimate shear forces for smaller widths (the effective width is not reached yet). After reaching a threshold, further increasing the width of the specimen will lead to the shear capacity remaining constant. A threshold is indeed observed experimentally (*27)* after an almost linear capacity increase for increasing. The resulting threshold width is compared to the calculated effective width from the load spreading methods, showing that the French method is to be preferred. Moreover, a statistical comparison between the experimental shear capacity (Delft experiments as well as slab database experiments) and the shear capacity from EN 1992-1-1:2005 based on b_{eff1} and b_{eff2} results in a better average and smaller coefficient of variation when using b_{eff2}. For wheel loads in the first lane, an asymmetric effective width can be used.

The minimum effective width can be taken as $4d_l$, provided that this value is a lower bound of:

$$1.3(1.5b_{load} + d_l + b_e) \tag{1}$$

with b_{load} = the width of the load, and b_e = the distance between the free edge and the center of the load.

Transverse Load Redistribution

To take into account the higher shear capacities of slabs, the introduction of an additional enhancement factor reducing the contribution of concentrated loads to the total shear force is proposed. The comparison between experimental results and calculated results based on EN 1992-1-1:2005 (*7*) and b_{eff2} results in a 5% lower bound for the enhancement factor of 1.25 for wheel loads close to the support.

In EN1992-1-1:2005 §6.2.2(6) the contribution to the shear force of a load applied within a distance $0.5d_l \leq a_v \leq 2d_l$ may be multiplied by $\beta = a_v/2d_l$ with a_v the face-to-face distance between the load and the support. For concentrated loads close to the support on slabs, β can be combined with the enhancement factor of 1.25 into $\beta_{new} = a_v/2.5d_l$ for $0.5d_l \leq a_v \leq 2.5d_l$.

Hypothesis of Superposition

The goal of S19 to S26 was to verify the hypothesis of superposition of shear stresses at the support for the shear stress τ_{conc} due to the concentrated load over the effective width b_{eff2} and the shear stress τ_{line} due to the distributed load over the full slab width, b. If the hypothesis holds true, then the sum of τ_{conc} and τ_{line} should not be smaller than the ultimate shear stress in an experiment with a concentrated load only, $\tau_{tot,cl}$, Fig. 4. The experimental results (Fig. 4b) confirm that the hypothesis of the superposition is a conservative assumption (*27*).

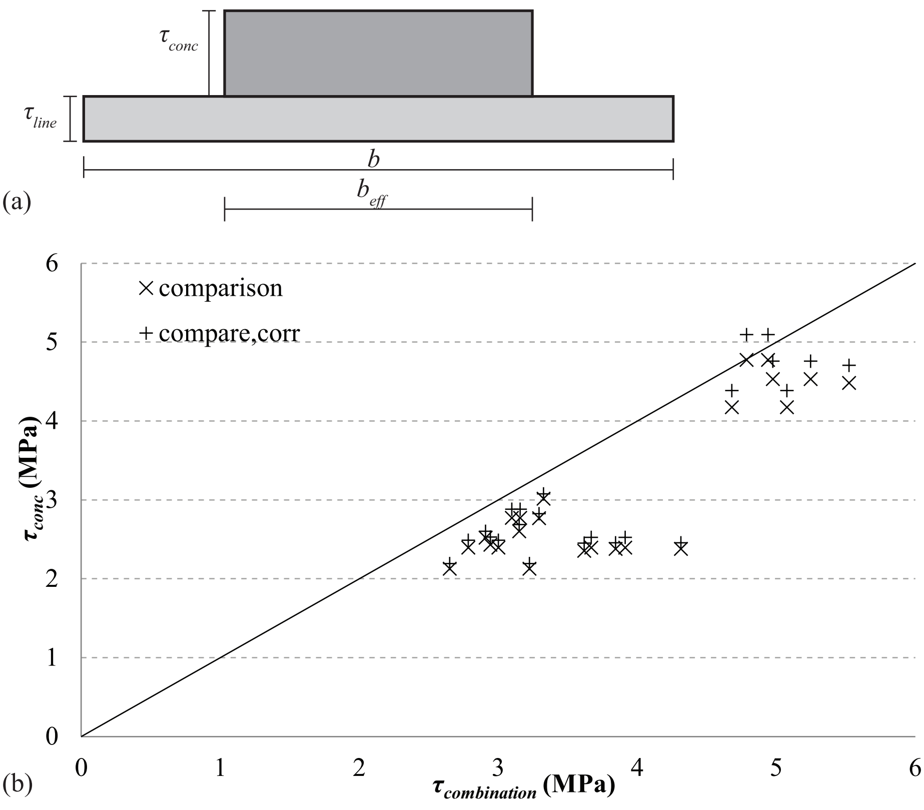

FIGURE 4 Superposition: (a) Principle of superposition of the shear stress due to a concentrated load over the effective width to the distributed load over the full slab width, (b) Experimental results comparing the shear capacity at the support due to a concentrated load only and due to a combination of a concentrated load and a line load. Compare,corr results are corrected for the difference in concentrated compressive strength.

Assumptions in Quick Scan sheet

As not all geometric and material properties are known for existing bridges, some assumptions for the Dutch bridge stock are stated here and applied within the scope of the Quick Scan method.

If no material testing data is available, the cube compressive strength of the concrete f_{cc} can be taken as 45MPa (6.5ksi). To assess the superimposed loads, the wearing surface is assumed to be 12cm (4.7in), leading to a fictitious tire contact area of 640mm × 640mm (25in × 25in) on the concrete surface as a result of vertical load distribution.

All trucks are assumed to be centered in their lane. The most unfavorable position to determine the maximum shear force at the edge is obtained by placing the first design truck such that the face-to-face distance between the support and the fictitious tire contact area equals $2.5d_l$. This distance is governing as load reduction can be used up to $2.5d_l$ with β_{new}. In the second and third lane, the design truck is placed such that the effective width associated with the first axle reaches up to the edge of the viaduct, Fig. 5, with:

a_{vi} the i^th^ face-to-face distance between the support and the tire contact area;
b_r the edge distance to the side of the first tire contact area, minimum 48cm (19in);
a_i the i^th^ center-to-center distance between the support and the tire contact area;
$b_{load} \times l_{load}$ the width and length of the tire contact area;
b_{effi} the i^th^ effective width;
i 1.. 6, corresponding to the considered axle.

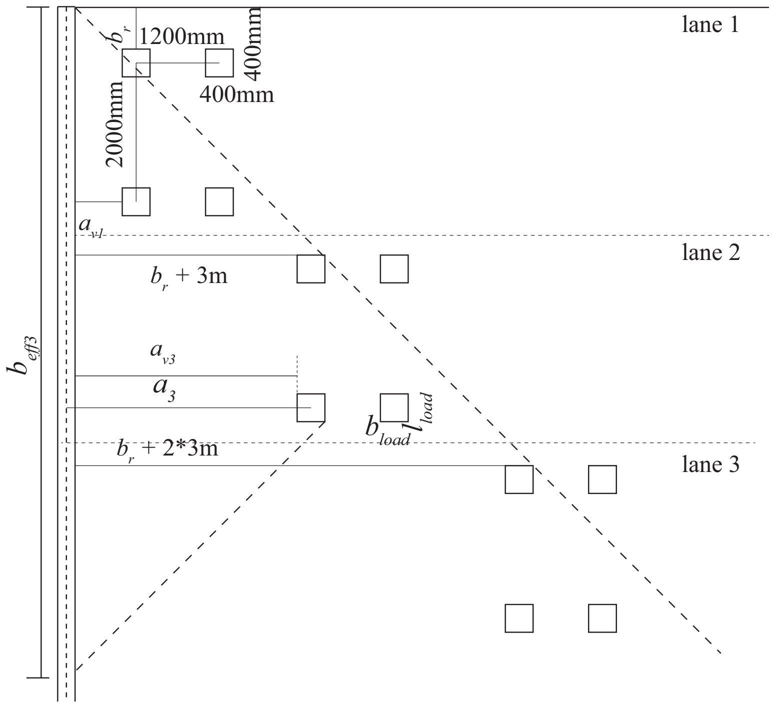

FIGURE 5 Most unfavorable position of the design trucks. Note: 1mm = 0.04in, 1m = 3.28ft

Results of case studies

Taking into account the recommendations from the research, the assumptions for the geometry and material properties and the provisions from the Eurocode suite, a Quick Scan spreadsheet (QS-EC) is developed. Similarly, a Quick Scan spreadsheet based on the AASHTO LRFD (*8*) and Manual of Bridge Evaluation (23) is developed (QS-AASHTO). Continuous slab bridges are checked at minimum 3 sections: the end support (sup 1-2), the end span near the mid support (sup 2-1) and the mid span near the mid support (sup 2-3).

The considered cases are 9 Dutch existing solid slab bridges that have insignificant skew angles, with at least 3 spans and an (almost) constant cross-sectional depth plus the example slab bridge (MBE A7) from the MBE (23). The properties are given in Table 2, with:

b width of the slab bridge;
d_l effective depth to the longitudinal reinforcement;
l_{span} span length;
f_{cc} concrete cube compressive strength;
ρ_l longitudinal reinforcement ratio.

TABLE 2 Properties of cases: 1 to 9 are existing bridges in the Netherlands, MBE A7 is the example from the Manual of Bridge Evaluation. Note: 1m = 3.28ft, 1MPa = 0.145ksi

Section	b (m)	d_l (m)	l_{span} (m)	f_{cc} (MPa)	ρ_l (%)
1 sup 1-2	9.6	0.791	9.505	45	0.443
1 sup 2-1	9.6	0.791	9.505	45	0.517
1 sup 2-3	9.6	0.791	13.007	45	0.517
1 sup 3-4	9.6	0.791	15.526	45	0.583
2 sup 1-1	14.45	0.331	7.04	45	1.045
2 sup 2-1	14.45	0.331	7.04	45	1.045
2 sup 2-3	14.45	0.331	8.38	45	1.045
3 sup 1-1	11.92	0.600	7.075	58.3	0.429
3 sup 2-1	11.92	0.600	7.075	58.3	0.429
3 sup 2-3	11.92	0.600	8.382	58.3	0.429
4 sup 1-1	11.92	0.360	7.075	70.6	0.716
4 sup 2-1	11.92	0.360	7.075	70.6	0.716
4 sup 2-3	11.92	0.360	8.382	70.6	0.716
5 sup 1-2	13.6	0.542	9.5	48.4	0.817
5 sup 2-1	13.6	0.542	9.5	48.4	0.909
5 sup 2-3	13.6	0.542	12.50	48.4	0.909
6 sup 1-2	19.2	0.457	10	49.6	0.934
6 sup 2-1	19.2	0.457	10	49.6	0.934
6 sup 2-3	19.2	0.457	13	49.6	0.934
7 sup 1-2	14.75	0.54	9.5	37.3	0.77
7 sup 2-1	14.75	0.54	9.5	37.3	1.284
7 sup 2-3	14.75	0.54	14	37.3	1.284
8 sup 1-2	13.36	0.59	12	66.4	1.366
8 sup 2-1	13.36	0.59	12	66.4	1.573
8 sup 2-3	13.36	0.59	15.05	66.4	1.573
9 sup 1-2	12.5	0.65	10	74.6	0.55
9 sup 2-1	12.5	0.65	10	74.6	1.092
9 sup 2-3	12.5	0.65	15	74.6	1.092
MBE A7	13.1	0.31	6.553	19.8	0.334

The results of the Quick Scans are given in Table 3, with:

v_{Ed}	shear force at the support as a result of composite dead load and live loads from EN 1991-2:2003 (*18*) load model 1;
$v_{Rd,c}$	shear capacity according to EN 1992-1-1:2005 (*7*).
uc EC	resulting unity check according to QS-EC;
v_u	shear force at the support as a result of composite dead load and live loads (governing case of lane load with design truck or with design tandem) according to AASHTO LRFD (*8*) and the MBE (23);
v_c	design shear capacity according to AASHTO LRFD (*8*);
uc AASHTO	resulting unity check according to QS-AASHTO.

TABLE 3 Results of 10 cases according to QS-EC and QS-AASHTO. Note: 1MPa = 0.145ksi

Section	v_{Ed} (MPa)	$v_{Rd,c}$ (MPa)	uc EC	v_u (MPa)	v_c (MPa)	uc AASHTO
1 sup 1-2	0.267	0.450	0.595	0.335	0.978	0.343
1 sup 2-1	0.401	0.473	0.847	0.452	0.812	0.557
1 sup 2-3	0.449	0.473	0.948	0.502	0.557	0.900
1 sup 3-4	0.517	0.493	1.048	0.580	0.557	1.041
2 sup 1-1	0.533	0.715	0.746	0.457	1.868	0.252
2 sup 2-1	0.715	0.715	0.999	0.603	1.105	0.559
2 sup 2-3	0.727	0.715	1.018	0.609	1.105	0.551
3 sup 1-1	0.280	0.534	0.524	0.310	1.237	0.250
3 sup 2-1	0.401	0.534	0.750	0.412	1.04	0.396
3 sup 2-3	0.403	0.534	0.755	0.398	1.04	0.382
4 sup 1-1	0.453	0.725	0.625	0.433	1.633	0.265
4 sup 2-1	0.618	0.725	0.853	0.554	1.398	0.408
4 sup 2-3	0.629	0.725	0.868	0.557	1.243	0.448
5 sup 1-2	0.444	0.615	0.723	0.454	1.379	0.329
5 sup 2-1	0.626	0.615	1.018	0.603	0.90	0.671
5 sup 2-3	0.640	0.615	1.041	0.640	0.782	0.819
6 sup 1-2	0.525	0.67	0.783	0.510	1.619	0.315
6 sup 2-1	0.722	0.67	1.077	0.684	1.095	0.624
6 sup 2-3	0.738	0.67	1.102	0.720	0.969	0.743
7 sup 1-2	0.437	0.553	0.789	0.444	1.297	0.343
7 sup 2-1	0.606	0.656	0.924	0.591	1.007	0.587
7 sup 2-3	0.680	0.656	1.037	0.699	0.846	0.826
8 sup 1-2	0.439	0.798	0.550	0.477	1.694	0.282
8 sup 2-1	0.639	0.837	0.763	0.656	1.316	0.499
8 sup 2-3	0.638	0.837	0.762	0.682	1.105	0.617
9 sup 1-2	0.372	0..773	0.481	0.407	1.39	0.293
9 sup 2-1	0.543	0.773	0.703	0.554	1.39	0.399
9 sup 2-3	0.609	0.773	0.788	0.657	1.016	0.647
MBE A7	0.674	0.423	1.596	0.576	0.853	0.675

The results of the calculations show similar shear forces for both QS-EC and QS-AASHTO (average of v_u/v_{Ed} = 1.01 with a standard deviation of 0.10). However, two remarks should be made: 1) the shear force due to the AASHTO loading incorporates the resistance factor φ = 0.9; and 2) the load factors from NEN 8700:2011 result in higher target reliability levels (β_{rel} = 3.6) as compared to AASHTO LRFR (β_{rel} = 2.5, the lower bound for loss of human life). Therefore, the limits of this comparison should be kept in mind.

AASHTO LRFD allows for higher shear capacities as compared to EN 1992-1-1:2005 (average of $v_c/v_{Rd,c}$ = 1.78 with a standard deviation of 0.41). Both methods take the size effect in shear into account, resulting in smaller shear capacities for larger depths. While EN 1992-1-1:2005 results in shear capacities of < 0.50 MPa for low levels of flexural reinforcement (ρ_l < 0.6%), the influence on the calculated shear capacities according to AASHTO LRFD is smaller. The smallest shear capacity according to AASHTO LRFD is obtained for a long span (l/d_l = 19.6). The viaducts with material research (f_{cc} > 55MPa) have higher shear capacities according to AASHTO LRFD as compared to EN 1992-1-1:2005. This observation is explained by noting that AASHTO (*8*) uses a square root for the compressive strength and EN 1992-1-1:2005 (*7*) a cube root.

The unity checks according to the QS-AASHTO are lower (on average 40%, standard deviation of 0.16) as compared to the QS-EC. With the QS-EC, 8 sections in 5 viaducts are identified as needing further investigations. With the QS-AASHTO, only 1 section remains. For only this case, QS-AASHTO results in a higher value for the unity check. The MBE-A7 example does not require shear to be checked according to the MBE (23), which is reflected by the small QS-AASHTO unity check value. However, when calculating this example with QS-EC a unity check value almost 2.4 times larger is found.

SUMMARY AND CONCLUSIONS

As a result of increased live loads and more conservative shear provisions in the recently implemented Eurocodes, a large number of the existing reinforced concrete solid slab bridges in the Netherlands are under discussion. To better assess their shear capacity, it is necessary to study the literature with regard to transverse load redistribution in slabs, the live load models and assessment practice. This literature study shows that experimental data on slabs under wheel loads close to the support is scarce. The Eurocode load model uses 3 design trucks with 2 closely spaced axles, leading to high shear forces at the support. The practice of assessment at the "repair" level in the Netherlands requires a higher target reliability index (β_{rel} = 3.8) than according to the "design-operating" level of the Manual of Bridge Evaluation (β_{rel} = 2.5).

To study the shear capacity of slabs under concentrated loads, a unique and extensive series of experiments is carried out. The results of these experiments are compared to the state-of-the-art on the shear capacity of beams. Slabs, unlike beams, show a transverse load redistribution that increases the shear capacity of slabs under concentrated loads close to the support as compared to beams. As a result, recommendations for the assessment of slab bridges are given:

- use the effective width resulting from the French horizontal load distribution method,
- with a minimum of $4d_l$;
- use a reduction factor $\beta_{new} = a_v/2.5d_l$ for $0.5d_l \leq a_v \leq 2.5d_l$ for wheel loads on slabs, and
- use superposition of stresses at the support for concentrated loads over the effective width with distributed loads over the full slab width.

To assess the large number of slab bridges under discussion in the Netherlands, a spreadsheet-based “Quick Scan” tool is developed, in which the recommendations based on the experimental research are implemented. Assumptions valid for the bridges owned by the Dutch Minsitry of Infrastructure and the Environment for the thickness of the wearing surface and the concrete compressive strength are used as input in a selection of 9 cases of existing bridges. Additionally an example slab bridge from the Manual of Bridge Evaluation is studied. These cases are analyzed through the Quick Scan method according to the Eurocode and the AASHTO, showing less conservative results when using live loads and the shear capacity from AASHTO.

ACKNOWLEDGEMENT

The authors wish to express their gratitude and sincere appreciation to the Dutch Ministry of Infrastructure and the Environment (Rijkswaterstaat) for financing this research work.

REFERENCES

1. Higgins, C., Daniels, T. K., Rosowsky, D. V., Miller, T. H. and Yim, S. C. Assessment and risk ranking of conventionally reinforced concrete bridges for shear. In *Transportation Research Record: Journal of the Transportation Research Board*, No. 1928, Transportation Research Board of the National Academies, Washington, D.C., 2005, pp. 110-117.
2. Walraven, J.C. Residual shear bearing capacity of existing bridges. *fib* Bulletin 57, *Shear and punching shear in RC and FRC elements; Proceedings of a workshop held on 15-16 October 2010 in Salò, Lake Garda, Italy*. International Federation for Structural Concrete (*fib*), Lausanne, Switzerland, pp. 129-138.
3. Cope, R. J. Flexural shear failure of reinforced concrete slab bridges. *Proceedings of the Institution of Civil Engineers Part 2-Research and Theory*, Vol. 79, No. SEP, 1985, pp. 559-583.
4. Azizinamini, A., Boothby, T. E., Shekar, Y. and Barnhill, G. Old concrete slab bridges: 1. Experimental investigation. *Journal of Structural Engineering – ASCE.* Vol. 120, No. 11, 1994, pp. 3284-3304.
5. Haritos, N., Hira, A., Mendis, P., Heywood, R., Giufre, A. Load testing to collapse limit state of Barr Creek Bridge. In *Transportation Research Record: Journal of the Transportation Research Board*, No. 1696, Transportation Research Board of the National Academies, Washington, D.C., 2000, pp. 92-102.
6. Aktan, A.E., Zwick, M., Miller, M. and Shahrooz, B. Nondestructive and Destructive Testing of Decommissioned Reinforced Concrete Slab Highway Bridge and Associated Analytical Studies. In *Transportation Research Record: Journal of the Transportation Research Board,* No. 1371, Transportation Research Board of the National Academies, Washington, D.C. 1992, pp. 142-153.
7. EN 1992-1-1:2005. *Eurocode 2 – Design of Concrete Structures: Part 1-1 General Rules and Rules for Buildings, EN 1992-1-1.* Comité Européen de Normalisation, Brussels, Belgium, 2005.
8. *AASHTO LRFD Bridge Design Specifications*, American Association of State Highway and Transportation Officials, Washington, DC, 2007

9. König, G. and Fischer, J. Model Uncertainties concerning Design Equations for the Shear Capacity of Concrete Members without Shear Reinforcement. *CEB Bulletin 224, "Model Uncertainties and Concrete Barrier for Environmental Protection"*, 1995, pp. 49-100.
10. Vecchio, F. J., and Collins, M. P. The Modified Compression-Field Theory for Reinforced Concrete Elements Subjected to Shear. *Journal of the American Concrete Institute*, Vol. 83, No. 2, 1986, pp. 219-231
11. Chauvel, D., Thonier, H., Coin, A., and Ile, N. *Shear Resistance of slabs not provided with shear reinforcement CEN/TC 250/SC 02 N 726*. 2007. France.
12. Sherwood, E. G., Lubell, A. S., Bentz, E. C., and Collins, M. P. One-way shear strength of thick slabs and wide beams. *ACI Structural Journal*, Vol. 103, No. 6, 2006, pp. 794-802.
13. Lantsoght, E.O.L., *Shear in reinforced concrete slabs under concentrated loads close to the support – Literature review*, Stevinrapport, Delft University of Technology, The Netherlands, 2012.
14. Regan, P. E. *Shear Resistance of Concrete Slabs at Concentrated Loads close to Supports*, Structures Research Group, Polytechnic of Central London, U.K. 1982.
15. Graf, O. Versuche über die Widerstandsfähigkeit von Eisenbetonplatten unter konzentrierter Last nahe einem Auflager. *Deutscher Ausschuss für Eisenbeton*, Vol. 73, 1933, pp. 10-16.
16. Richart, F. E. and Kluge, R. W., Tests of reinforced concrete slabs subjected to concentrated loads: a report of an investigation, *University of Illinois Engineering Experiment Station Bulletin No. 314*, V. 36, No. 85, University of Illinois, Urbana, 1939.
17. Cullington, D. W., Daly, A. F., and Hill, M. E. Assessment of reinforced concrete bridges: Collapse tests on Thurloxton underpass. *Bridge Management*, Vol. 3, 1996, pp. 667-674.
18. EN 1991-2:2003. *Eurocode 1 – Actions on Structures - Part 2: Traffic loads on bridges, EN 1991-2*, Comité Européen de Normalisation, Brussels, Belgium, 2003.
19. NEN 8700:2011. *Assessment of existing structures in case of reconstruction and disapproval - Basic Rules, NEN 8700*, Nederlands Normalisatieinstituut, Delft. 2011.
20. Steenbergen, R., Vrouwenvelder, T., Scholten, N. Veiligheidsfilosofie bestaande bouw. *Cement*. Vol. 64, No. 4, 2012, pp. 8-16.
21. Steenbergen, R. D. J. M., and Vrouwenvelder, A. C. W. M. Safety philosophy for existing structures and partial factors for traffic loads on bridges. *Heron*, Vol. 55, No. 2, 2010, pp. 123-140.
22. EN 1990:2002. *Eurocode 0 – Basis of structural design, EN 1990* , Comité Européen de Normalisation, Brussels, Belgium. 2002.
23. AASHTO. *Manual for Bridge Evaluation (AASHTO LRFR*) American Association of State Highway and Transportation Officials, Washington D.C. 2011.
24. Ghosn, M., Sivakumar, B., and Miao, F. Calibration of Load and Resistance Factor Rating Methodology in New York State. In *Transportation Research Record: Journal of the Transportation Research Board,* No. 2200, Transportation Research Board of the National Academies, Washington, D.C., 2010, pp. 81-89.
25. Lantsoght, E.O.L., van der Veen, C., and Walraven, J. Shear capacity of slabs and slab strips loaded close to the support. *SP287 – Recent Developments in Reinforced Concrete Slab Analysis, Design and Serviceability*, 2012, pp. 5.1-5.17.
26. Lantsoght, E.O.L., van der Veen, C., and Walraven, J. Shear tests of reinforced concrete slabs and slab strips under concentrated loads. *Proceedings of the 9th fib International PhD Symposium in Civil Engineering*, Karlsruhe, Germany, 2012, pp. 3-8.

27. Lantsoght, E.O.L., van der Veen, C., and Walraven, J. Shear assessment of solid slab bridges. *Proceedings of ICCRRR 2012, 3rd International Conference on Concrete Repair, Rehabilitation and Retrofitting*, Cape Town, South Africa, 2012, pp. 827-833.